

# Direct Numerical Simulation of Single Bubble Rising in Viscous Stagnant Liquid

Nima. Samkhaniani, Azar. Ajami, Mohammad Hassan. Kayhani, Ali. Sarreshteh Dari

**Abstract**— In this paper, direct numerical simulation of two-phase incompressible gas-liquid flow is presented. The interface between two-phase is tracked with Volume of Fluid (VOF) method with Continuous Surface Force (CSF) model. Newtonian flows are solved using a finite volume scheme based on the Pressure Implicit with Splitting of Operators (PISO) algorithm. The results of two test cases are presented to assess the correctness of OpenFOAM CFD package codes. First test case includes a single spherical bubble in liquid, extra pressure produced in bubble is compared with Young – Laplace equation, in second case, dynamic of bubble is investigated by comparing the frequency of oscillating elliptic bubble with Lamb equation. Then the terminal Reynolds numbers and shapes of isolated gas bubbles rising in quiescent liquids are compared with data taken from the bubble diagram of Grace.

**Keywords**—Bubble Rising, Direct Numerical Simulation, OpenFOAM, Volume Of Fluid.

## I. INTRODUCTION

MULTIPHASE flows occur in a wide range of situations such as many important biological and industrial processes and they have been extensively studied by researchers both theoretically and experimentally. One very fundamental example of multiphase flows is that of a single gas bubble rising and deforming in a viscous liquid. It is clear a thorough knowledge of this basic system is of major importance to understand more complex flows such as bubbly flows. Numerous experiments [1-3] have been studied single bubbles rising in stagnant or motion liquids, however, despite its apparent simplicity important aspects of the behavior of a single bubble rising in stagnant liquid still remain uncertain.

The rise of a bubble in liquid is a function of several parameters such as bubble characteristics (size and shape), properties of gas-liquid systems (density, viscosity, surface tension, concentration of solute, density difference between gas and liquid), liquid motion (direction), and operating conditions (temperature, pressure, gravity).

Some limitations in experimental methods make numerical investigation necessary, for example it is difficult to get complete information about the flow field and pressure distribution in the entire domain or the bubble rising is affected by solute and bubble initial formation [1].

In recent years, direct numerical simulations and interface tracking methods contribute to a better physical understanding of multiphase flows. The great advantage of numerical simulations is that they avoid some of the aforementioned practical difficulties encountered in experiments. The rising of a bubble gas in quiescent liquid have been studied several times since now [4-8], in this paper at first the correctness of OpenFOAM CFD package [9] is validated, then it is applied to a single bubble rising problem, and terminal velocity and bubble shapes are compared with grace regime map [2].

## II. NUMERICAL MODEL

The mass conservation equation for incompressible fluid flow in entire domain is:

$$\nabla \cdot \mathbf{u} = 0 \quad (1)$$

Two phases are immiscible, and there is an interface between them. Material properties and the flow field are discontinuous across the interface between the fluids. The interface is not defined as a sharp boundary and a transition region exist where the fluid is treated as some mixture of the two fluids on each side of the interface. The local material properties of the fluid are defined in:

$$\beta(x, t) = \beta_L + (\beta_G - \beta_L)\alpha(x, t) \quad (2)$$

Where  $\beta$  represents density ( $\rho$ ) and viscosity ( $\mu$ ), and  $\alpha$  is void fraction which is the ratio of one fluid volume to the cell volume.

$$\alpha(\vec{x}) = \frac{V_{phase1}}{V} = \begin{cases} 1 & \vec{x} \in \text{phase1} \\ 0 < \alpha < 1 & \vec{x} \in \text{interface} \\ 0 & \vec{x} \in \text{phase2} \end{cases} \quad (3)$$

Interface moves at the velocity of “ $u$ ” so gas and liquid have the same velocity at interface and there is no shear stress there. The equation for the advection of the phase field variable is:

$$\frac{D\alpha}{Dt} = \frac{\partial \alpha}{\partial t} + \mathbf{u} \cdot \nabla \alpha = 0 \quad (4)$$

OpenFOAM uses an extra artificial compression term to limit the solution of  $\alpha$  equation between zero and one.

Nima. Samkhaniani is Ph.D student in Engineering and Technology Department, Tarbiat Modares University. (e-mail: nima.samkhaniani@modares.ac.ir)

Azar. Ajami is M.S student in Mechanical Engineering Department, Shahrood University of Technology. (e-mail: ajamy.mech88@yahoo.com)

Mohammad Hassan. Kayhani is associate professor in Mechanical Engineering Department, Shahrood University of Technology. (e-mail: m\_kayhani@yahoo.com).

Ali. Sarreshtehdari is assistant professor in Mechanical Engineering Department, Shahrood University of Technology. (e-mail: sarreshtehdari@tus.ac.ir)

$$\frac{\partial \alpha}{\partial t} + \nabla \cdot (U \alpha) + \nabla \cdot (U_r \alpha (1 - \alpha)) = 0 \quad (5)$$

The artificial term is only active in the thin interface region because of the multiplication term  $\alpha(1 - \alpha)$ .  $U_r$  is a velocity field suitable to compress the interface [10].

Using the continuum surface force model (CSF), the momentum transport equations for incompressible flow are:

$$\frac{\partial}{\partial t}(\rho u) + \nabla \cdot (\rho u u) = -\nabla P + \nabla \cdot [\mu(\nabla u + \nabla u^T)] + \rho g + \sigma \kappa \nabla \alpha \quad (6)$$

In above equations,  $\sigma$  and  $\kappa$  are the surface tension and curvature of interface, respectively. Curvature of the phase interface is:

$$\kappa = \nabla \cdot \left( \frac{\nabla \alpha}{|\nabla \alpha|} \right) \quad (7)$$

### III. DIRECT NUMERICAL METHODS

Various numerical methods for direct simulation of two phases (gas – liquid) system have been implemented since now. VOF, Level-Set, and Front-Tracking are three leading methods among interface tracking methods. These methods can be divided within two main groups: Lagrangian techniques and Eulerian techniques, depending on the way the interfaces are described.

Front-Tracking method [11] is the most accurate way to simulate two phase flow; it uses two grids for simulation, fixed grid for computation of flow field and moving grid for tracking interface accurately. However, it is computationally high. This method belongs to Lagrangian techniques.

Eulerian techniques use a scalar function to define the location of the interface. VOF [12] and Level-Set method [13] belong to this group. Level-Set is based on a smooth distance function whose zero value corresponds to the location of the interface. Level Set techniques classically suffer from poor mass. VOF uses fraction of one of the fluids, a property varying sharply from 0 to 1 across the interfacial region. It conserves mass in incompressible fluid and also it is not computationally high. These characters make VOF the most popular interface tracking method. In fact, in VOF method, the motion of the interface is not tracked, but rather the volume of each material in each cell is evolved in time that is why sometimes it has been called volume tracking methods [14]. For tracking interface exactly and sharply in each cell, an interface reconstruction algorithm is needed. This step is based on the local volume fraction and the orientation of its gradient. VOF has been developed through last three decades extensively; it can be classified based on surface reconstruction method. SLIC and PLIC are two well-known VOF methods. A historical review of VOF methods evolution can be found in References [14-16].

OpenFOAM does not use any geometric tools to reconstruct interface, so interface, here is not a line anymore, and it is a region. In OpenFOAM, VOF suffers from interface smearing. In Fig 1 interface can be in any cells of A, B or C. An interface

compression method has been implemented in this code to reduce surface smearing[10]. Surface tension is uniform along interface. Constant surface force (CSF) model [12] is used here, eliminates need for surface reconstruction for calculation of surface tension and it simplifies calculation and enables accurate modeling of two and three dimensional modeling.

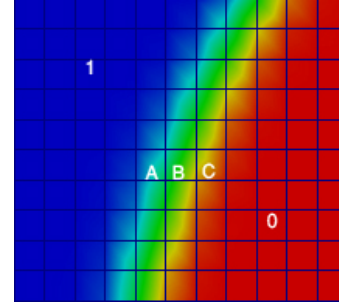


Fig 1: Interface smearing

### IV. RESULT AND DISCUSSION

As a first step, VOF model is subjected to several tests (static and dynamic) to verify the correctness of the code implementation. In first test the implementation of the surface tension model is tested by comparing the computed pressure jump with the Young–Laplace equation, then an ellipsoidal bubble is simulated as a dynamic test and numerical result is compared with lamb analytical result. Following these tests, shapes and rise velocities of gas bubbles are compared with the corresponding data obtained from the bubble diagram published by Grace [2].

#### A. NUMERICAL MODEL VALIDATION STATIC TEST

It is well known that surface tension induces an excess pressure inside a bubble which for a spherical bubble can be calculated from the Youngs –Laplace equation:

$$\Delta P = \frac{2\sigma}{R} \quad (8)$$

Physical properties and simulation setup information are presented in table I. Fig 2 shows the spherical bubble which is positioned in the center of the grid domain in a zero gravity field.  $u$ ,  $p$ , and  $\alpha$  are zero gradient at boundary conditions.

TABLE I  
SIMULATION DATA FOR STATIC TEST

Computational grid	80×80×80	-
Grid	0.0005	m
Bubble radius	0.01	m
Liquid density	1000	kg/m <sup>3</sup>
Gas density	10	kg/m <sup>3</sup>
Dynamic viscosity (liquid, gas)	1×10 <sup>-4</sup>	m/s <sup>2</sup>
Surface tension	1	N/m

Error can be estimated by the following equation, where  $P_1$  and  $P_2$  are the mean pressure inside and outside of bubble, respectively:

$$Error = \frac{(P_1 - P_2) - \Delta P}{\Delta P} \quad (9)$$

Simulations are done on different grid size; grid size 0.05 mm shows around 9% underestimate in pressure jump calculation.

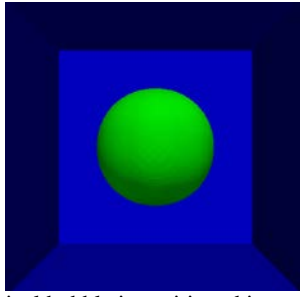


Fig 2 Spherical bubble is positioned in stagnant liquid

In Fig 3 the computed pressure distribution in a vertical plane cutting through the center of the bubble is compared to the analytical solution.

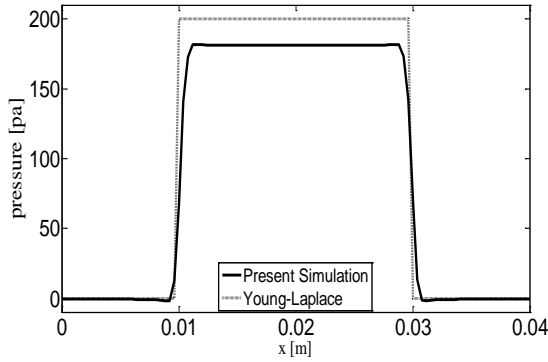


Fig 3 Pressure distribution

### B. DYNAMIC TEST

An elliptic bubble in a zero gravity field, starting to oscillate due to surface tension, it is a good starting point to simulate dynamic behavior of bubble rising. To check on the accuracy of computed results, the period of oscillations is compared with the analytical solution obtained for small perturbation of a column of liquid with zero viscosity provided by Lamb:

$$w_0^2 = m(m-1) \frac{\sigma}{\rho_L R_{eq}^3} \quad (10)$$

$R_{eq}$ ,  $m$ , and  $\omega_0$  are mean bubble radius, oscillation mode, and frequency. Oscillation mode is 2 here. Frequency of the oscillation is related to the period of oscillation ( $T_0 = 2\pi/\omega_0$ ).  $R_{eq}$  is the radius of a circle which its area is equivalent with computed elliptic bubble, and is defined in:

$$R_{eq} = \sqrt{R_L \times R_s} \quad (11)$$

For dynamic test, physical properties and simulation setup information are presented in Table II.

TABLE II

SIMULATION DATA FOR DYNAMIC TEST

Computational grid	100×100	-
Grid	0.0004	<i>m</i>
Aspect ratio ( $R_L/R_s$ )	2	-
Bubble large radius ( $R_L$ )	0.01	<i>m</i>
Liquid density	1000	kg/m <sup>3</sup>
Gas density	10	kg/m <sup>3</sup>
Viscosity (liquid, Gas)	1×10 <sup>-7</sup>	m/s <sup>2</sup>
Surface tension	0.1	N/m

The bubble is positioned in the centre of the simulation surface.  $u$ ,  $p$ , and  $\alpha$  are zero gradient at boundary conditions. Fig 4 shows bubble shape evolution for a period, the aspect ratio (large diameter/small diameter) is 2.

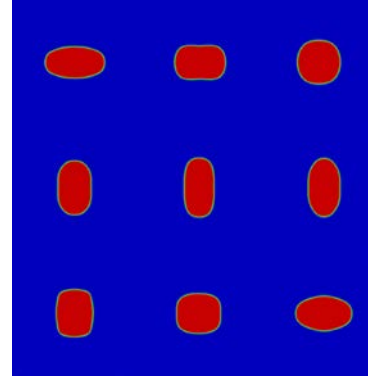


Fig 4 Ellipse bubble oscillation shape in a period

In Lamb equation, increasing the aspect ratio will increase bubble frequency. Similar behavior is observed in numerical simulation for various aspect ratios (Fig 5).

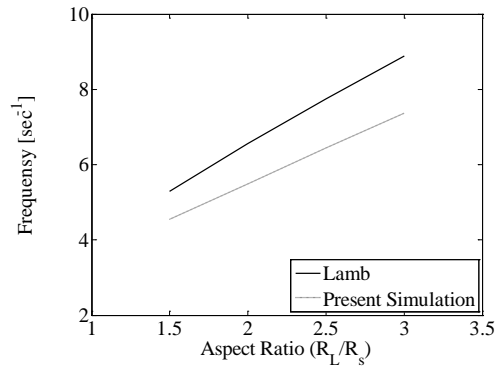


Fig 5 bubble frequencies over aspect ratio

Viscosity force damps bubble motion, so if viscosity increases, bubble motion stops faster, and it becomes circular sooner. In Fig 6, position of one point on interface is shown for two different viscosity values.

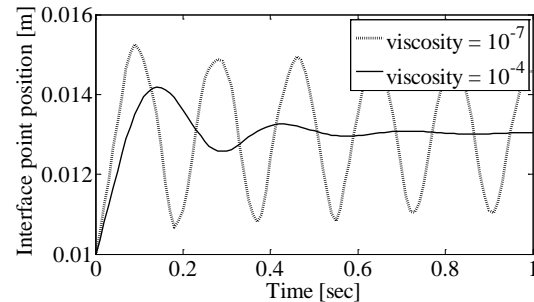


Fig 6 one point oscillation on interface

Relative error is computed in:

$$relative\ Error = \frac{100(w - w_0)}{w_0} \quad (12)$$

Result shows a large error, around 40 percent between analytical and computational frequencies. However, this large error is in the range of other similar implemented code [18].

### C. BUBBLE RISING

Air bubble due to buoyancy rises in stagnant liquid. Bubble interface evolution is affected by body force and surface force. Based on experimental results, different bubble shapes are distinguished as a function of the Eötvös, Morton, and Reynolds numbers [2]:

$$E_o = \frac{g \Delta \rho d^2}{\sigma}, M_o = \frac{g \Delta \rho \mu^4}{\rho^2 \sigma^3}, Re = \frac{\rho d u_T}{\mu} \quad (13)$$

$d$  and  $u_T$  are mean bubble diameter and terminal velocity. To reduce the computational cost, the axisymmetric computational domain with  $80 \times 400$  grids is chosen for bubble rising simulation. Width of domain on the bubble radius is 1.50 and the height is 4 of width. Axisymmetric domain, boundary conditions and  $\alpha$  field initial condition is shown in Fig 7.

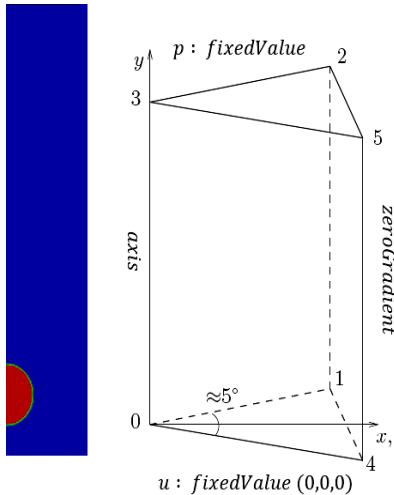


Fig 7 Boundary condition and  $\alpha$  field initial condition

Bubble velocity is the slope of the bubble gravity center displacement. Bubble rapidly reaches its terminal velocity. Terminal velocity shows the balance of force on bubble. In Fig 8 displacement of dimpled ellipsoidal bubble is shown which reaches its terminal velocity in less than 0.2 second. For other bubble shapes, there are similar graph. Reynolds ( $Re_c$ ) are computed and compared with experimental result ( $Re$ ) in Table III.

TABLE III  
DATA FOR BUBBLE RISING MODELING

Models	$\Delta t(sec)$	$d(mm)$	$E_o$	$\log(M)$	$Re$	$Re_c$
1 Spherical	0.08	1.50	0.35	-3.9	1	1.02
2 Dimpled ellipsoidal	0.4	32.0	160	3.5	1.5	0.89
3 Ellipsoidal	0.1	8.0	10	-2.1	12	8.34
4 Skirted	0.25	62.0	600	2.2	23	18.24
5 Wobbling	0.03	4.0	2.5	-11.8	2000	1834
6 Spherical cap	-	45.0	320	-7.6	4200	3765

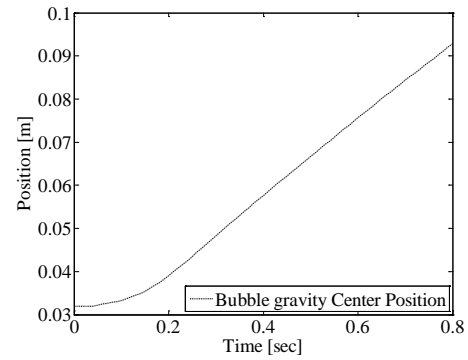


Fig 8 displacement of gravity center of dimpled ellipsoidal bubble

Bubble evolution is shown in Fig 9 and compared with grace regime map in Fig 10. Result shows good agreement in several shapes like spherical bubble. Unfortunately, this numerical model could not simulate spherical cap shape. High Reynolds number causes it breaks so fast in numerical model. Of course computed Reynolds of departed bubble is near to the experimental result but there is no shape similarity by grace regime map.

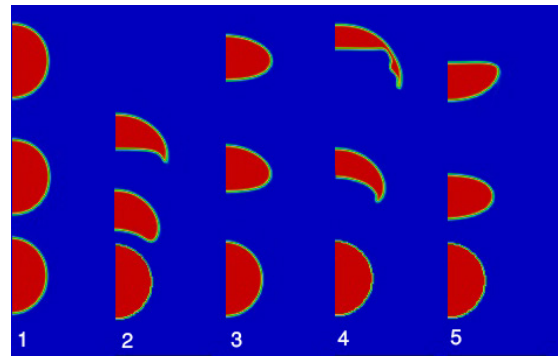


Fig 9 Different bubble shapes

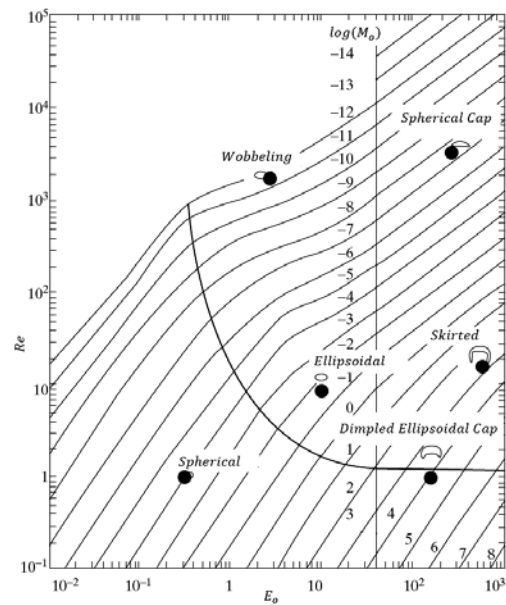


Fig 10 Grace Regime map (● present simulation)

The difference among numerical and empirical results can be divided in two main groups: 1) Numerical limitations and simplification such as interface curvature estimations, constant surface tension assumption or straight trajectory assumption, 2) Empirical uncertainty such as purity of experimental fluid, effect of tiny particle on bubble shape, and so on.

In highly Reynolds number bubble rising, such as spherical cap bubble, assumption of straight trajectory is not totally accepted, and experimental data show bubble passes the spiral path around a vertical axis [18], so this phenomena needs a fully 3D simulation, and axisymmetric simulation is not suggested.

## V.CONCLUSIONS

In this Article, OpenFOAM CFD package is used to modeling bubble rising in stagnant liquid. Through article, direct numerical methods are introduced generally and governing Equations and method which OpenFOAM solves two-phase flow in one fluid model is implied specifically. The correctness of solver was shown with two simple case tests, and then solver was applied to simulate the rise of bubble.

For simulation of air bubble rising, several assumptions such as axisymmetric shape and straight trajectory were made. Comparing numerical result with empirical data showed good agreement both quantitatively and qualitatively in most bubble regime map but for high Reynolds bubble regime, straight trajectory was not good assumption. Also, numerical investigation showed, computational domain width are enough to be just 2 or 3 times of bubble largest diameter to make the assumption of infinite domain true.

## REFERENCES

- [1] A. A. Kulkarni, and J. B. Joshi, "Bubble Formation and Bubble Rise Velocity in Gas-Liquid Systems: A Review". Ind. Eng. Chem. Res, vol. 44, pp.5873-5931, 2005.
- [2] R. Clift, J. R Grace, and M. E. Weber, *Bubbles, Drops, and Particles*. Academic Press. London. 1978, pp.27.
- [3] D. Rodrigue, "A general correlation for the rise velocity of single gas bubbles" Can. J. Chem. Eng., vol.82 (2), pp. 382-386, 2004
- [4] M.Koebe, and D. Bothe, Pruess, J., and Warnecke, H. J., "3D direct numerical simulation of air bubbles in water at high Reynolds number", Proceedings ASME Fluids Engineering Division Summer Meeting. 2002
- [5] F. Raymond, and J. M. Rosant, "A numerical and experimental study of the terminal velocity and shape of bubbles in viscous liquids", Chem. Eng. Sci. vol. 55, pp. 943-955, 2000.
- [6] J. Dai, J. D. Sterling, and A. Nadim, 2004 "Numerical simulation of air bubbles in water using an axisymmetric VOF method", Advances in Fluid Mechanics: Computational Methods in Multiphase Flow II. WIT Press.
- [7] D. Lrstad, and L. Fuchs, "High-order surface tension VOF-model for 3D bubble flows with high density ratio", J. Comput. Phys. vol. 200, pp. 153-176, 2004
- [8] M.van Sint Annaland, N.G. Deen ,and J.A.M. Kuipers , "Numerical simulation of gas bubbles behaviour using a three-dimensional volume of fluid method", Chemical Engineering Science, vol 60, pp. 2999 – 3011, 2005
- [9] H. G. Weller, G. Tabor,I.H. Jasak, and C. Fureby, "A tensorial approach to computational continuum mechanics using object-oriented techniques", Computers In Physics, vol.12, pp.620-632,1998
- [10] E. Berberović, N.P. van Hinsberg, S. Jakirlić, I.V. Roisman, and C. Tropea, "Drop impact onto a liquid layer of finite thickness: Dynamics of the cavity evolution", The American Physical Society, vol.79, pp.036306 (15), 2009.
- [11] S. Unverdi, and G. Tryggvason, "A front-tracking method for viscous, incompressible multi-fluid flows". J. Comput. Phys. vol. 100, pp. 25–37, 1992.
- [12] J.U. Brackbill, D.B. Kothe, and C. Zemach, "A continuum method for modeling surface tension" J. Comput. Phys. vol.100, pp. 335–354. 1992.
- [13] M. Sussman , E. Fatemi, P. Smereka, S. Osher, "An improved level set method for incompressible two-phase flows" Comput. Fluids 27, 663–680, 1998.
- [14] Rider, W.J., and D.B. Kothe, "Reconstructing volume tracking". Journal of Computational Physics, 1998
- [15] D.J. Benson, "Volume of fluid interface reconstruction methods for multi-material problems". Appl Mech Rev, vol 55, no 2, March 2002
- [16] R. Scardovelli, and Zaleski, "Direct numerical simulation of free-surface and interfacial flow" Annu. Rev. Fluid Mech, vol. 31, pp. 567–603, 1999
- [17] M. Seifollahi, E. Shirani, N. Ashgriz, "An improved method for calculation of interface pressure force in PLIC-VOF methods", European Journal of Mechanics B/Fluids, vol. 27, pp. 1–23, 2008
- [18] J. Hua, P. Lin, and J.F. Stene, "Numerical Simulation of Gas Bubbles Rising in Viscous Liquids at High Reynolds Number", 6th International Conference on Multiphase Flow, Leipzig, Germany, July 9 - 13, 2007